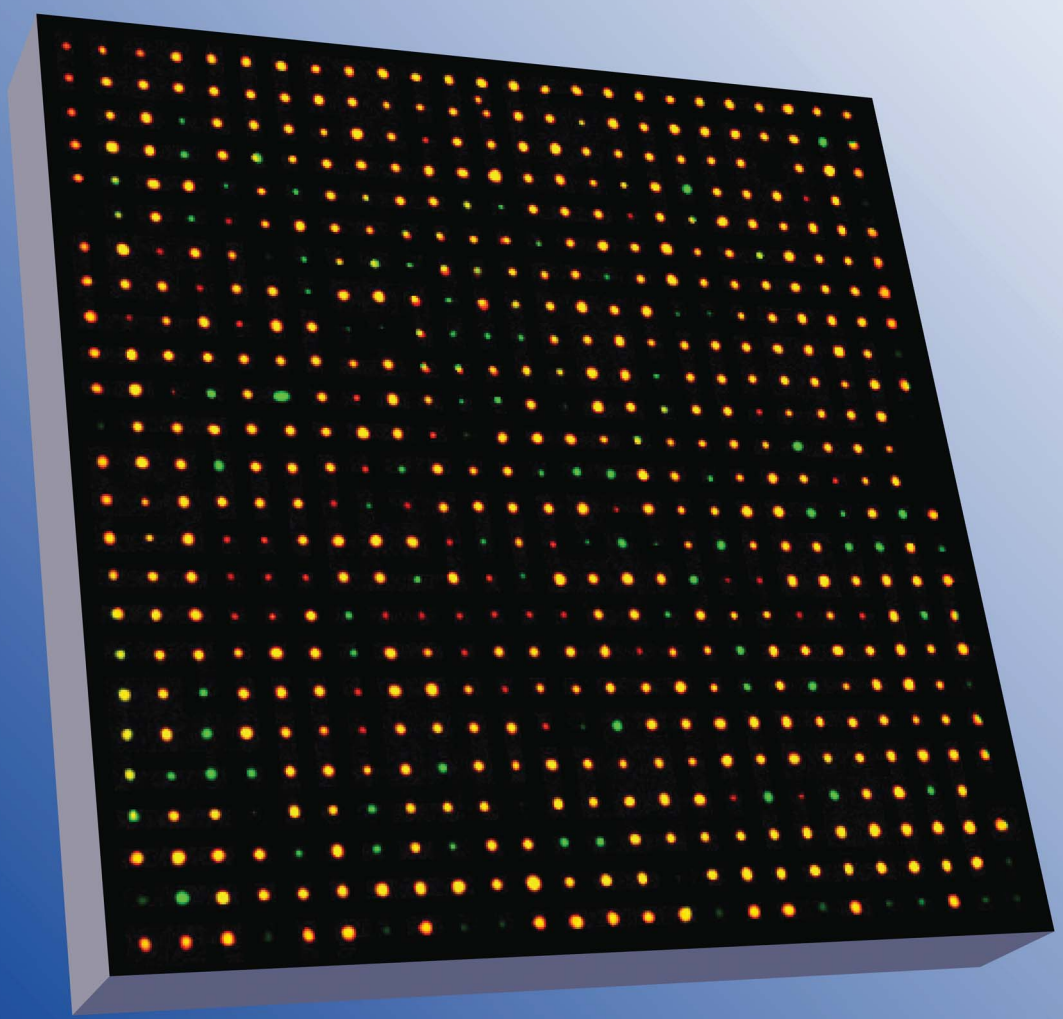
Nanoscale

www.rsc.org/nanoscale

Volume 4 | Number 2 | 21 January 2012 | Pages 309–672



ISSN 2040-3364

COVER ARTICLE

Xu *et al.*

High-throughput ultrasensitive characterization of chemical, structural and plasmonic properties of EBL-fabricated single silver nanoparticles

RSC Publishing

NCNST

2040-3364(2012)4:2;1-O

View Online / Journal Homepage / Table of Contents for this issue
Dynamic Article Links

Nanoscale

Cite this: *Nanoscale*, 2012, **4**, 380

www.rsc.org/nanoscale

COMMUNICATION

High-throughput ultrasensitive characterization of chemical, structural and plasmonic properties of EBL-fabricated single silver nanoparticles†

Tao Huang,‡[a] Wei Cao,‡[b] Hani E. Elsayed-Ali*[bc] and Xiao-Hong Nancy Xu*[a]

Received 22nd September 2011, Accepted 4th November 2011
DOI: 10.1039/c1nr11368b

Published on 25 November 2011 on http://pubs.rsc.org | doi:10.1039/C1NR11368B
Downloaded by Old Dominion University on 11 January 2012

Electron beam lithography (EBL) has become a popular means to prepare a wide variety of nano-arrays for numerous studies and applications, including photonics and sensors. Their fabrications and characterizations are costly and time consuming, underscoring the importance of developing effective tools to rapidly study their physicochemical stabilities and properties over time. In this study, we characterized EBL-fabricated single silver nanoparticle (Ag NP) arrays over their 12-week exposure to ambient conditions using SEM/EDS, AFM and dark-field optical microscopy and spectroscopy (DFOMS). We found that chemical compositions, structural morphologies and plasmonic optical properties of single NPs altered drastically over the exposure. Single cuboid and triangular-prism Ag NPs degraded at rates of (0.74 ± 0.02) and (0.66 ± 0.02) per week, and their localized surface plasmon resonance (LSPR) spectra showed striking blue-shifts (171 ± 25 and 203 ± 35 nm) over the 12-week exposure, respectively. Plasmonic colors of single NPs changed distinctively from red to green over the 12-week exposure. The LSPR spectra of individual NPs in each array were acquired simultaneously and correlated specifically with their SEM and AFM images, demonstrating that DFOMS can serve as high-throughput, ultrasensitive and non-invasive means to characterize chemical, structural and optical properties of nano-arrays *in situ* in real time at single-NP resolution.

Noble metal NPs (*e.g.*, Ag NPs) show distinctive optical and electronic properties and their potential unique applications in nanoelectronics, nanophotonics, nanosensors, and nanomedicines.[1–6] EBL can precisely control sizes and shapes of individual NPs, as well as inter-NP spaces and their array configurations. Thus, EBL has been widely used to fabricate nano-arrays with desired sizes, shapes and configurations for a wide variety of applications.[6–10] Although EBL has been used to fabricate Ag NP arrays, few studies characterize chemical and morphological stabilities of Ag NP arrays and probe their effects on LSPR spectra of individual NPs.[6,11,12]

Chemical degradations of Ag metals and thin films under ambient conditions and their related mechanisms (*e.g.*, tarnishing and corrosion of Ag due to formation of Ag_2S, silver sulfide) have been extensively studied over decades.[13–16] Studies showed that carbonyl sulfide (OCS) and hydrogen sulfide (H_2S), commonly present in the atmosphere, were involved in creation of Ag_2S on the surface of Ag.[13–15] High humidity in the atmosphere also served as a primary factor to enhance the sulfidation processes and led to generation of both sulfate and Ag_2S.[14] The formation of Ag_2S on the surface of EBL-fabricated Ag NPs was suggested to alter dielectric environments of NPs and led to the red-shifts of plasmonic absorption spectra of NP arrays over their brief exposure to the air.[11]

In our previous studies, we found that EBL-fabricated Ag NP arrays underwent drastic chemical and morphological degradations over their weeks of exposure to the atmosphere.[12] However, when the arrays were stored under vacuum (6×10^{-2} Torr), they remained stable over months.[12] The results also showed that high energy electron beams of high-resolution SEM/EDS affected and sometimes destroyed surface morphologies of single NPs, which prevented the same NPs from being continuously investigated over time using SEM.[12] Such interesting findings underscore the importance of developing non-invasive means to effectively characterize nano-arrays. Furthermore, SEM/EDS and AFM cannot provide photonic properties of individual NPs, limiting the possibility of exploring optical applications of nano-arrays.

It is worth noting that single Ag NPs that were fabricated by nanosphere lithography (NSL) and immediately stored in vacuum desiccators remained stable over months.[17] Furthermore, purified colloidal Ag NPs that were synthesized by reducing Ag^+ with reducing agents (*e.g.*, $NaBH_4$ and sodium citrate), thoroughly washed and suspended in deionized (DI) water, and stored at 4 °C, were extremely stable.[18–21] We used such wet-synthesis Ag NPs for several previous studies over years, and we did not observe chemical, morphological and optical degradations of single NPs, as characterized by HRTEM and DFOMS.[18–21] Our findings suggest that functional groups (*e.g.*, citrate and PVP) adsorbed on Ag NPs may prevent the formation of Ag_2S on their surfaces and thereby protect NPs from degradations. Thus, one can take appropriate measures (*e.g.*, storing nano-arrays under vacuum or functionalizing their surfaces) to maintain the stability of NPs over desired periods of time.

[a]*Department of Chemistry and Biochemistry, Old Dominion University, Norfolk, VA, 23529, USA. E-mail: xhxu@odu.edu; Fax: +1 (757) 683-5698; Tel: +1 (757) 683-5698*
[b]*Applied Research Center, Old Dominion University, Norfolk, VA, 23529, USA. E-mail: helsayed@odu.edu; Fax: +1 (757) 269-5644; Tel: +1 (757) 269-5645*
[c]*Department of Electrical and Computer Engineering, Old Dominion University, Norfolk, VA, 23529, USA*
† Electronic supplementary information (ESI) available. See DOI: 10.1039/c1nr11368b
‡ Both authors contributed equally to this work.

This journal is © The Royal Society of Chemistry 2012

Published on 25 November 2011 on http://pubs.rsc.org | doi:10.1039/C1NR11368B
Downloaded by Old Dominion University on 11 January 2012

To achieve enormous potential applications of EBL-fabricated nano-arrays, it is essential to: (i) prepare single NP arrays that maintain chemical, structural and optical properties of individual NPs for any desired period of time; and (ii) develop high-throughput, ultrasensitive and non-invasive means to effectively and rapidly characterize individual NPs *in situ* in real time. To these ends, in this study, we used EBL to fabricate 25 × 25 single Ag NP arrays on microscopic glass slides coated with indium tin oxide (30 nm thickness): one array with square-shaped NPs (each cuboid NP has a length (L_s) of 312 ± 8 nm and height (H_s) of 45 ± 4 nm), and the other array with triangular shaped NPs (each triangular-prism has a length (L_t) of 283 ± 10 nm and height (H_t) of 45 ± 4 nm). We then exposed the arrays to ambient conditions (45–55% relative humidity; air-conditioned dark room; 25 °C) over 12 weeks, and characterized chemical, morphological and LSPR properties of single NPs in each array over the 12-week exposure using SEM/EDS, AFM and DFOMS.

SEM images of single Ag NP arrays in Fig. 1 and 2 show drastic morphological changes of single NPs over their 12-week exposure to the ambient conditions. The 3 × 3 array (representative portion of the 25 × 25 array) of squared Ag NPs in Fig. 1 and their zoom-in images in Fig. 2A and B show that the surface of NPs became rougher, and four sharp corners of squared NPs vanished and became rounded. Notably, NPs were broken apart to loose pieces of smaller cylindrical (disk-shaped) clusters, each with diameters (D_s) of 35 ± 5 nm and heights (H_{sd}) of 25 ± 7 nm, over their 12-week exposure to the atmosphere.

Similar phenomena were observed for EBL-fabricated triangular Ag NP arrays (Fig. 2C and D). The images show that the NP was broken to smaller cylindrical (disk-shaped) clusters, each with diameters (D_t) of 41 ± 7 nm and heights (H_{td}) 27 ± 8 nm, and three sharp corners (tips) of the triangular NP were vanishing and became truncated, suggesting the size and surface-area dependent degradation kinetics. The portions of NPs with smaller sizes and larger surface areas (sharper corners) are subject to faster degradation.

To investigate degradations of single NPs at three dimensions (3D), we characterized the heights and lengths of single NPs in the arrays using AFM. The representative AFM image of a single triangular NP in Fig. 3 shows extremely rough surfaces with wide ranges of heights after the 12-week exposure in (B), which is in contrast with the smooth surface (nearly identical height) of the same NP freshly fabricated by EBL in (A). The images also show that the lengths and heights of the NP shrank dramatically and the sharp tips of the NP were disappearing and became truncated over the 12-week exposure.

EDS analysis of single Ag NPs on the nano-arrays showed the presence of a significant amount of sulfur on the surface of NPs after their 12-week exposure to the atmosphere. The ratio of Ag to S at 3.2 was determined, suggesting the formation of Ag_2S on the surface of NPs, as we reported previously.[12]

The formation of Ag_2S could cause the NPs to break to tiny clusters due to significant lattice mismatch between Ag and its sulfide. Ag metal is crystallized in the face-centered cubic structure with a lattice constant of 4.090 Å, while Ag_2S at room temperature has a monoclinic lattice with each sulfur atom surrounded by four Ag atoms with each spaced at 2.475, 2.511, 2.547, and 2.563 Å.[22] This significant mismatch between the lattice structures of Ag and Ag_2S creates interfacial stress that can break NPs to smaller clusters, which

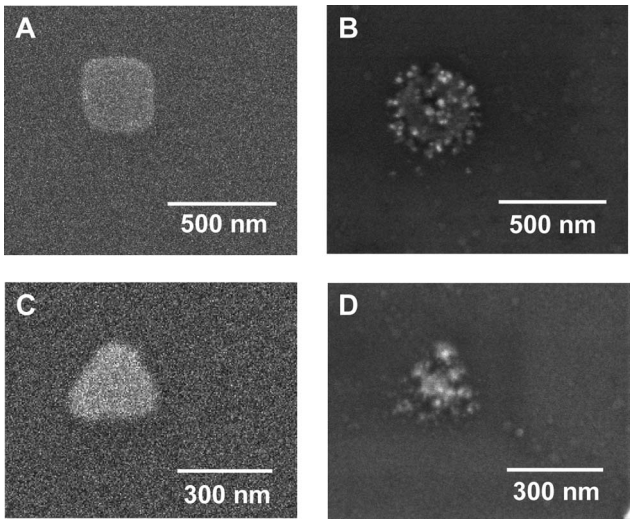


Fig. 2 Zoom-in SEM images of representative Ag NPs on the 25 × 25 arrays, similar to those in Fig. 1: (A) square-shaped (cuboid) and (C) triangular-prism NPs, as freshly fabricated by EBL; (B) the NP of (A) and (D) the NP of (C), after their 12-week exposure to the atmosphere, show extreme degradations of the NPs, which were broken down to smaller clusters and their sizes shrunk dramatically over the exposure.

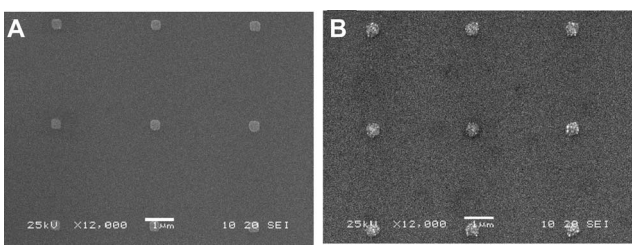


Fig. 1 SEM images of single square-shaped (cuboid) Ag NP arrays: (A) as freshly fabricated by EBL and (B) after their 12-week exposure to the atmosphere (45–55% relative humidity; air-conditioned dark room; 25 °C), show drastic morphological changes of single NPs over the exposure. The 3 × 3 array shows the portion of the entire 25 × 25 array.

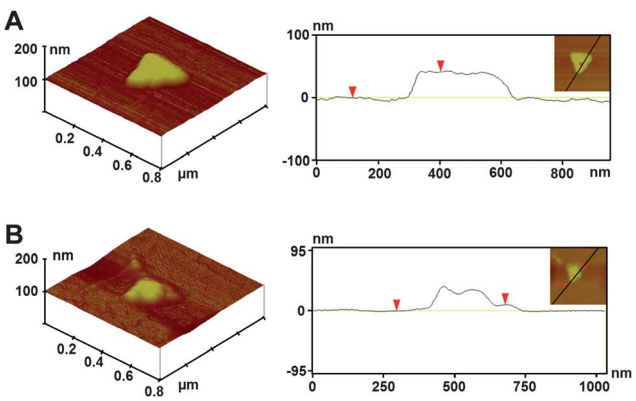


Fig. 3 AFM images of the representative single triangular Ag NP on the arrays: (A) as freshly fabricated by EBL and (B) after 12-week exposure to the atmosphere, show drastic degradations in 3D and a rough surface with various heights ranging from 10 to 40 nm.

Published on 25 November 2011 on http://pubs.rsc.org | doi:10.1039/C1NR11368B
Downloaded by Old Dominion University on 11 January 2012

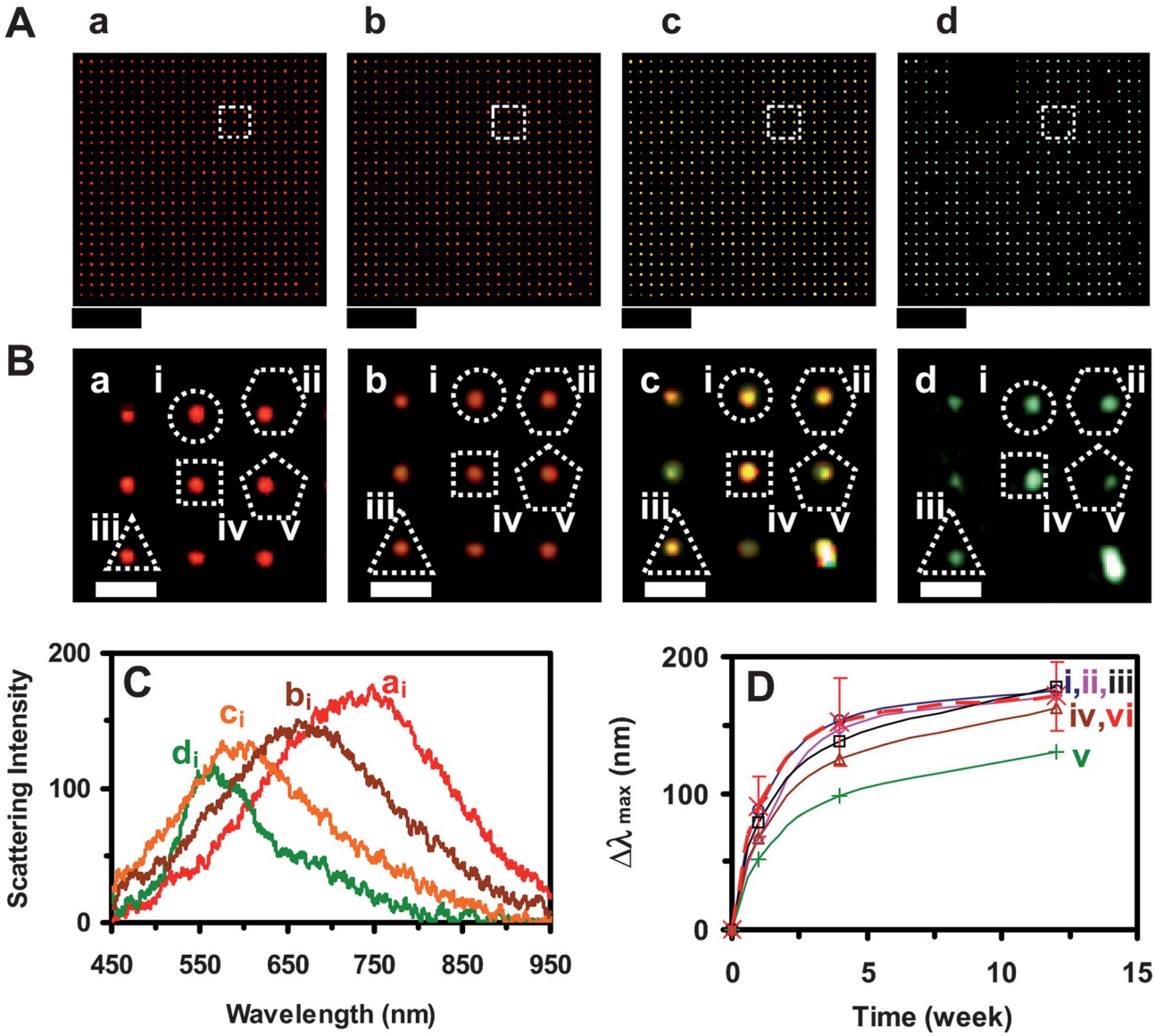


Fig. 4 Dark-field optical images and LSPR spectra of single square-shaped NPs on the arrays: (A) 25 × 25 arrays and (B) 3 × 3 arrays of (A) over: (a) 0, (b) 1, (c) 4, and (d) 12 weeks exposure to the atmosphere. (C) LSPR spectra of the NP labeled by (i) in (B) show its λ_{max} (FWHM) of: (a_i) 750 (239), (b_i) 662 (205), (c_i) 596 (168), and (d_i) 575 (127) nm, over: (a_i) 0, (b_i) 1, (c_i) 4, and (d_i) 12 weeks of exposure. (D) Plots of blue shifts ($\Delta\lambda_{max}$) of LSPR spectra of the NP labeled by (i–v) in (B), and (vi) average λ_{max} of LSPR spectra of single NPs on the entire 25 × 25 array *versus* their exposure time to the atmosphere show that the $\Delta\lambda_{max}$ increases rapidly with time during the first 4 weeks of exposure and gradually reaches the plateau over the additional 8 weeks of exposure. The plots show the first-order degradation reactions as fitted by $\Delta\lambda_{max} = 166 \times (1 - e^{-0.735t})$ with $R^2 = 0.996$ and average rate constants (k) of 0.74 ± 0.02 per week. Scale bars are 20 μm in (A) and 4 μm in (B). See enlarged images of (A) in Fig. S3†.

explains our observations (Fig. 1–3). For instance, why Ag NPs degraded over their exposure to the ambient conditions and why sharper corners of single NPs degraded faster than the bulk, which are attributed to their larger surface area and higher amount of Ag_2S.

We characterized the degradation of EBL-fabricated Ag NP arrays *in situ* in real time using DFOMS. Dark-field optical images and LSPR spectra of individual NPs on the entire 25 × 25 arrays in Fig. 4 and 5 show profound alterations of plasmonic colors (blue-shifts of LSPR spectra) of individual NPs from red to green over their 12-week exposure to the atmosphere.

Peak wavelengths (λ_{max}) of LSPR spectra of single square-shaped NPs on the array freshly fabricated by EBL (Fig. 4 and S1 in the ESI†) range from 718 to 762 nm with full-width-at-half-maximum (FWHM) from 226 to 247 nm, showing that none of the single NPs on the array is identical. For example, LSPR spectra of freshly fabricated single NPs labeled as (i–v) in (B) show distinctive λ_{max} (FWHM) of 750 (239), 733 (245), 738 (202), 720 (214), and 692 (207) nm (Fig. 4C and S1†), respectively. The result indicates underlying variations of individual NPs in nano-arrays and demonstrates ultrasensitive detection capabilities of DFOMS. The average λ_{max} and FWHM of LSPR spectra of individual NPs on the entire array are (746 ± 21) and (238 ± 9) nm, respectively.

Over their 12-week exposure to the atmosphere (Fig. 4C and D), their average λ_{max} shifts to 575 ± 15 nm and their average FWHM

 This journal is © The Royal Society of Chemistry 2012

Published on 25 November 2011 on http://pubs.rsc.org | doi:10.1039/C1NR11368B
Downloaded by Old Dominion University on 11 January 2012

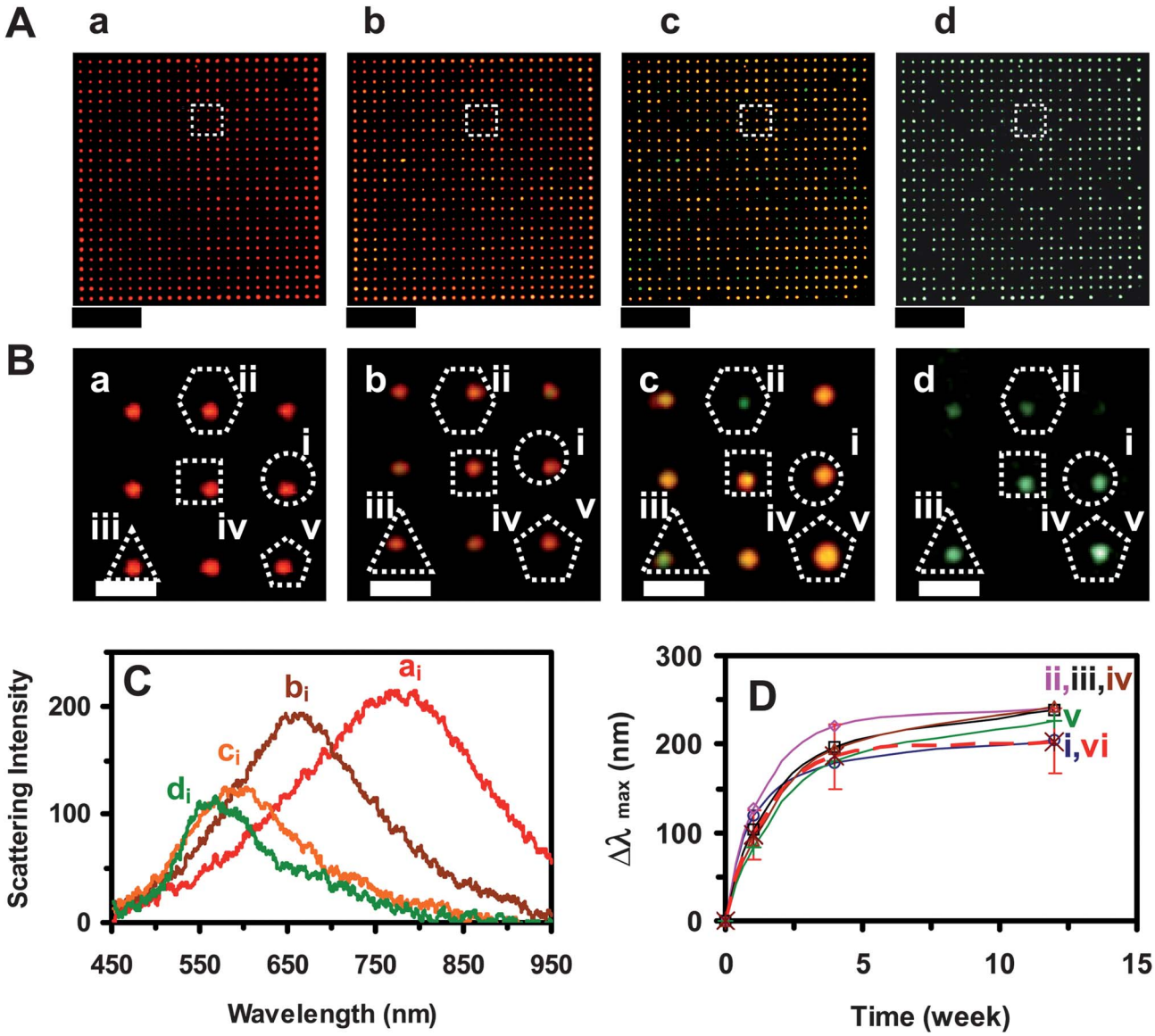


Fig. 5 Dark-field optical images and LSPR spectra of single triangular NPs on the arrays: (A) 25 × 25 arrays and (B) 3 × 3 arrays of (A) over: (a) 0, (b) 1, (c) 4, and (d) 12 weeks of exposure to the atmosphere. (C) LSPR spectra of single NPs labeled as (i) in (B) show its λ_{max} (FWHM) of: (a_i) 782 (261), (b_i) 662 (215), (c_i) 603 (172), and (d_i) 577 (133) nm over: (a_i) 0, (b_i) 1, (c_i) 4, and (d_i) 12 weeks exposure. (D) Plots of the blue shifts ($\Delta\lambda_{max}$) of LSPR spectra of the NP labeled as (i–v) in (B), and (vi) average λ_{max} of LSPR spectra of single NPs on the entire 25 × 25 array *versus* their exposure time to the atmosphere show that the $\Delta\lambda_{max}$ increases rapidly with time during the first 4 weeks of exposure and gradually reaches the plateau over the additional 8 weeks of exposure. The plots show the first order degradation reactions as fitted by $\Delta\lambda_{max} = 202 \times (1 - e^{-0.656t})$ with $R^2 = 0.999$ and average rate constants (k) of 0.66 ± 0.02 per week. Scale bars are 20 μm in (A) and 4 μm in (B) See enlarged images of (A) in Fig. S4†.

narrows to 128 ± 11 nm, with the ranges of 558–588 nm for λ_{max} and 117–135 nm for FWHM. The result shows gigantic blue shifts of λ_{max} of single NPs by (171 ± 25) nm with their FWHM reduced by (110 ± 19) nm, leading to striking plasmonic color changes of single NPs from red to green.

Notably, plasmonic images of single squared NPs on the same array (Fig. 4B and C and S1†) show multiple colors with various LSPR spectra at each given exposure time. Single red, orange, orange-yellow, yellow, yellow-green, and green NPs in the same array were observed at their 4th week of exposure to the atmosphere (Fig. 4C). The results show that each NP on the same array has its own degradation rate. For instance, λ_{max} (FWHM) of the LSPR spectrum of five representative single NPs: (i) NP (Fig. 4C) shifts from 750 (239) to 662 (205), 596 (168), and 575 (127) nm, with $\Delta\lambda_{max}$ (ΔFWHM) of 88 (34), 154 (71), and 175 (112) nm; (ii) NP (Fig. S1A†) shifts from 733 (245) to 666 (185), (586) (162), and 561 (126) nm, with $\Delta\lambda_{max}$ (ΔFWHM) of 67 (60), 147 (83), and 172 (119) nm; (iii) NP (Fig. S1B†) shifts from 738 (202) to 659 (187), 600 (169), and 560 (127) nm, with $\Delta\lambda_{max}$ (ΔFWHM) of 79 (15), 138 (33), and 178 (75) nm; (iv) NP (Fig. S1C†) shifts from 720 (214) to 653 (179), 595 (161), and 558 (122) nm, with $\Delta\lambda_{max}$ (ΔFWHM) of 67 (35), 125 (53), and 162 (92) nm; (v) NP (Fig. S1D†) shifts from 692 (207) to 641 (188), 594 (163), and 562 (125) nm, with $\Delta\lambda_{max}$ (ΔFWHM) of 51 (19), 98 (44), and 130 (83)

Published on 25 November 2011 on http://pubs.rsc.org | doi:10.1039/C1NR11368B
Downloaded by Old Dominion University on 11 January 2012

nm, over their one-week, 4-week and 12-week exposure to the air, respectively.

Plots of $\Delta\lambda_{max}$ (blue shifts) of single squared NPs *versus* their exposure time to the ambient conditions in Fig. 4D show that their $\Delta\lambda_{max}$ increases rapidly with time during the first 4 weeks of exposure, then gradually reaches the plateau over the additional 8 weeks of exposure. The blue-shift rates reflect the degradation rates of single NPs on the array, which follow the first-order reaction with a degradation rate of (0.74 ± 0.02) per week.

Taken together, the results in Fig. 4 indicate that each squared NP degrades and changes its plasmonic colors at its own distinct rates, which are most likely attributed to their various structural morphologies and surface roughnesses as originally fabricated by EBL. Conventional thin-film deposition techniques, which typically generate high degrees of defects, have been widely used by EBL. Therefore, the EBL-fabricated Ag NPs show high density and high degrees of defects, which lead to formation of diverse clusters of Ag_2S and various degradation rates of individual NPs.

Similar phenomena were observed for the triangular NPs (Fig. 5 and S2†). The λ_{max} of LSPR spectra of single triangular NPs in the 25 × 25 array freshly fabricated by EBL ranges from 766 to 795 nm with their FWHM of 252–273 nm. The average λ_{max} and FWHM of LSPR spectra of individual NPs in the entire array are (781 ± 18) and (263 ± 10) nm, respectively. Notably, over their 12-week exposure to the atmosphere, their average λ_{max} blue shifts to (578 ± 17) nm and their average FWHM shrinks to (131 ± 15) nm with 560–592 nm for λ_{max} and 118–137 nm for FWHM. The results show enormous blue shifts ($\Delta\lambda_{max}$) of single NPs by (203 ± 35) nm with their FWHM reduced by (132 ± 23) nm, which causes plasmonic color changes of single NPs from red to green.

Plasmonic images and LSPR spectra of single triangular NPs in the same array (Fig. 5 and S2†) show that individual NPs change colors (blue-shifts of their LSPR spectra) gradually, from red to orange, yellow, then green, over the 12-week exposure. Multiple colors of single NPs, such as red, red-orange, orange-yellow, yellow, yellow-green, and green NPs, in the array, were observed at their 4th week of exposure, which are most likely attributed to their various structural morphologies and surface roughnesses initially fabricated by EBL, as discussed above. The results further demonstrate ultra-sensitive capabilities of DFOMS and underscore the importance of characterization of nano-arrays at single NP resolution.

The results show that each NP on the same array displays a distinctive LSPR spectrum at each given exposure time, and has its own degradation rates. For example, λ_{max} (FWHM) of the LSPR spectrum of: (i) NP (Fig. 5C) shifts from 782 (261) to 662 (215), 603 (172), and 577 (133) nm, with $\Delta\lambda_{max}$ (ΔFWHM) of 120 (46), 179 (89), and 205 (128) nm; (ii) NP (Fig. S2A†) shifts from 801 (263) to 674 (218), (581) (169), and 561 (141) nm, with $\Delta\lambda_{max}$ (ΔFWHM) of 127 (45), 220 (94), and 240 (122) nm; (iii) NP (Fig. S2B†) shifts from 795 (258) to 691 (215), 599 (183), and 557 (144) nm, with $\Delta\lambda_{max}$ (ΔFWHM) of 104 (43), 196 (75), and 238 (114) nm; (iv) NP (Fig. S2C†) shifts from 793 (252) to 701 (212), 598 (185), and 551 (143) nm, with $\Delta\lambda_{max}$ (ΔFWHM) of 92 (40), 195 (67), and 242 (109) nm; (v) NP (Fig. S2D†) shifts from 774 (255) to 691 (188), 593 (183), and 548 (146) nm, with $\Delta\lambda_{max}$ (ΔFWHM) of 83 (67), 181 (72), and 226 (109) nm, over their one-week, 4-week and 12-week exposure to the air, respectively.

Plots of $\Delta\lambda_{max}$ of single triangular NPs *versus* their exposure time to the atmosphere in Fig. 5D show that $\Delta\lambda_{max}$ increases with time rapidly for the first 4 weeks of exposure, and gradually reaches the maximum during the additional 8 weeks of exposure. The blue-shift rates indicate the degradation rates of single NPs, which follow the first-order reactions with a degradation rate of (0.66 ± 0.02) per week. Optical images of both arrays (Fig. 4 and 5) also show that some of the NPs completely vanished from the arrays over the 12-week exposure, indicating their extreme rapid degradation and their removal from the surface during characterizations.

The corners of each array on the microscope slides were marked with four different symbols by EBL. These distinct symbols were easily recognized by SEM, AFM and DFOMS, and they guided us to identify and characterize the same NPs using these three imaging means. This simple approach enables us to locate any given single NPs in the array, and characterize the same NP in each array using SEM, AFM and DFOMS. LSPR spectra of single NPs in the arrays (Fig. 4 and 5) were specifically correlated with 3D morphological and chemical characterization of the same individual NPs of interest using SEM/EDS and AFM (Fig. 1–3), which enabled us to study their chemical and morphological dependent LSPR spectra, and to explain the huge blue-shifts and smaller FWHM of their LSPR spectra over the 12-week exposure.

As described by theories and previous studies,[21,23–27] LSPR spectra of single Ag NPs depend upon their sizes, shapes and surrounding environments (*e.g.*, dielectric constants of NPs and their embedded medium). Under electromagnetic fields (radiation of light), free electrons on the surface of smaller NPs oscillate at higher frequency than larger NPs. Thereby, smaller NPs display shorter wavelength of LSPR spectra than larger NPs. The removal (snipping) of sharp corners (tips) of the square-shaped and triangular NPs also led to the blue-shifts of their primary LSPR spectra, which resulted from dipole plasmon resonances related to in-plane polarization, as reported previously.[17,23] Single NPs (L_s = 312 ± 8 nm, H_s = 45 ± 4 nm; L_t = 283 ± 10 nm, H_t = 45 ± 4 nm) freshly fabricated by EBL were broken to loose pieces of much smaller disk-shaped NPs (D_s = 35 ± 5 nm, H_{sd} = 25 ± 7 nm; D_t = 41 ± 7 nm, H_{td} = 27 ± 8 nm) without sharp corners of cuboids and triangles (Fig. 2 and 3), which led to tremendous blue-shifts of LSPR spectra of single NPs (Fig. 4 and 5). The smaller NPs had a shorter dephasing time ($T2$) than larger NPs, which led to the smaller FWHM (narrower) of LSPR spectra.[28]

Unlike Ag NPs, Ag_2S clusters (semiconductors) do not possess high density of free electrons on their surface, and hence do not generate intense LSPR. The formation of Ag_2S on the surface of Ag NPs decreases reflectivity of NPs and alters dielectric constants of the surrounding medium of Ag NPs, which leads to the lower intensity and small red-shifts of LSPR spectra of single Ag NPs.[11] Such red-shift contributions are insignificant and overwhelmed by the primary contributions of blue-shifts of LSPR spectra due to the disintegration of large NPs to loose pieces of smaller NPs.

Taken together, the huge blue-shifts and smaller FWHM of LSPR spectra of individual Ag NPs (Fig. 4 and 5) are attributed to the decrease of their sizes due to disintegrations of larger NPs to tiny disk-shaped clusters upon their 12-week exposure to the ambient conditions.

Notably, LSPR spectra of every NP in an array (*e.g.*, 512 × 512) as large as the pixel array of a CCD camera can be characterized simultaneously at millisecond (ms) temporal and nanometer (nm) spatial resolutions using our DFOMS. The DFOMS is equipped with a microscope halogen lamp as the illuminator, which provides low intensity of dark-field illumination (0.070 ± 0.001 Watt) on the

 This journal is © The Royal Society of Chemistry 2012

nano-arrays (dark-field focal plane).[4,29,30] The high temporal resolution of DFOMS enables high-throughput characterization of individual NPs in nano-arrays and the minimal exposure of nano-arrays to the light, which makes characterization of nano-arrays rapid and minimally invasive. These distinct powerful capabilities of DFOMS make it unrivaled by any other existing characterization means.

In summary, we have used EBL to fabricate arrays of single Ag NPs with two distinct shapes (cuboid and triangular-prism). We have studied chemical, structural and optical properties and degradations of single NPs over their 12-week exposure to the atmosphere using SEM/EDS, AFM and DFOMS. The results show drastic changes of chemical, morphological and optical properties of single NPs over the exposure. The severe degradations of the EBL-fabricated Ag NPs to smaller disk-shaped clusters are most likely attributed to the formation of Ag_2S on the surface of NPs during the exposure. Their extreme degradations and subsequent disintegrations to loose pieces of tiny NPs led to enormous blue-shifts of LSPR spectra of single NPs. This study demonstrates that DFOMS is the most effective and non-invasive means to achieve high-throughput ultrasensitive characterization of chemical, morphological and optical properties of single NPs *in situ* in real time for a wide variety of applications (*e.g.*, screening of defects and degradations of single NP arrays over time).

Acknowledgements

This work is supported in part by NSF (NIRT: CBET 0507036) and NIH (R01 GM076440). EBL fabrication, SEM and AFM characterization were performed at the Applied Research Center, and DFOMS imaging and characterization of single NP arrays were carried out in the Xu's lab.

References

1 E. Ozbay, *Science*, 2006, **311**, 189–193.
2 M. K. Teli, S. Mutalik and G. K. Rajanikant, *Curr. Pharm. Des.*, 2010, **16**, 1882–1892.
3 X.-H. N. Xu and R. P. Patel, in *Encyclopedia of Nanoscience and Nanotechnology*, ed. H. S. Nalwa, American Scientific Publishers, Stevenson Ranch, CA, 2004, vol. 7, pp. 189–192.
4 T. Huang and X.-H. N. Xu, *Nanoscale*, 2011, **3**, 3567–3572.
5 T. Huang, P. D. Nallathamby and X.-H. N. Xu, *J. Am. Chem. Soc.*, 2008, **130**, 17095–17105.
6 J.-L. Bijeon, G. Barbillon, J. Plain, M. Lamy de la Chapelle, P.-M. Adam and P. Royer, *Surf. Sci.*, 2007, **601**, 5057–5061.
7 M. Baba, T. Sano, N. Iguchi, K. Iida, T. Sakamoto and H. Kawaura, *Appl. Phys. Lett.*, 2003, **83**, 1468–1470.
8 J. Zhao, X. Zhang, C. R. Yonzon, A. J. Haes and R. P. Van Duyne, *Nanomedicine*, 2006, **1**, 219–228.
9 J. L. Pearson and D. R. S. Cumming, *Microelectron. Eng.*, 2005, **78–79**, 343–348.
10 Z. Zhou and S. H. Lee., *Appl. Opt.*, 2008, **47**, 3177–3184.
11 M. Mcmahon, R. Lopez, H. M. Meyer, L. C. Feldman and R. F. Haglund, *Appl. Phys. B: Lasers Opt.*, 2005, **80**, 915–921.
12 W. Cao and H. E. Elsayed-Ali, *Mater. Lett.*, 2009, **63**, 2263–2266.
13 H. E. Bennett, R. L. Peck, D. K. Burge and J. M. Bennett, *J. Appl. Phys.*, 1969, **40**, 3351–3360.
14 T. E. Graedel, J. P. Franey, G. J. Gualtieri, G. W. Kammlott and D. L. Malm, *Corros. Sci.*, 1985, **25**, 1163–1180.
15 J. P. Franey, G. W. Kammlott and T. E. Graedel, *Corros. Sci.*, 1985, **25**, 133–143.
16 D. K. Burge, J. M. Bennett, R. L. Peck and H. E. Bennett, *Surf. Sci.*, 1969, **16**, 303–320.
17 Y. Song, P. D. Nallathamby, T. Huang, H. Elsayled-Ali and X.-H. N. Xu, *J. Phys. Chem. C*, 2010, **114**, 74–81.
18 T. Huang and X.-H. N. Xu, *J. Mater. Chem.*, 2010, **20**, 9867–9876.
19 K. J. Lee, P. D. Nallathamby, L. M. Browning, C. J. Osgood and X.-H. N. Xu, *ACS Nano*, 2007, **1**, 133–143.
20 P. D. Nallathamby, K. J. Lee and X.-H. N. Xu, *ACS Nano*, 2008, **2**, 1371–1380.
21 P. D. Nallathamby, T. Huang and X.-H. N. Xu, *Nanoscale*, 2010, **2**, 1715–1722.
22 A. B. Gordienko, Y. N. Zhuravlev and B. N. Fedorov, *Russ. Phys. J.*, 2006, **49**, 893–894.
23 K. L. Kelly, E. Coronado, L. L. Zhao and G. C. Schatz, *J. Phys. Chem. B*, 2003, **107**, 668–677.
24 G. Mie, *Ann. Phys.*, 1908, **25**, 377–445.
25 C. F. Bohren and D. R. Huffman, *Absorption and Scattering of Light by Small Particles*, Wiley, New York, 1983, pp. 287–380.
26 U. Kreibig and M. Vollmer, *Optical Properties of Metal Clusters*, Springer, Berlin, 1995, pp. 14–123.
27 P. Mulvaney, *Langmuir*, 1996, **12**, 788–800.
28 F. Hubenthal, *Prog. Surf. Sci.*, 2007, **82**, 378–387.
29 P. D. Nallathamby, K. J. Lee, T. Desai and X.-H. N. Xu, *Biochemistry*, 2010, **49**, 5942–5953.
30 X.-H. N. Xu, J. Chen, R. B. Jeffers and S. V. Kyriacou, *Nano Lett.*, 2002, **2**, 175–182.

Published on 25 November 2011 on http://pubs.rsc.org | doi:10.1039/C1NR11368B
Downloaded by Old Dominion University on 11 January 2012

Electronic Supplementary Material (ESI) for Nanoscale
This journal is © The Royal Society of Chemistry 2011

On-Line Supporting Information

High-Throughput Ultrasensitive Characterization of Chemical, Structural and Plasmonic Properties of EBL-Fabricated Single Silver Nanoparticles

Tao Huang,[a¥] Wei Cao,[b¥] Hani E. Elsayed-Ali,[b,c*] and Xiao-Hong Nancy Xu,[a*]

Departments of Chemistry and Biochemistry,[a] Applied Research Center,[b] and Electrical and Computer Engineering,[c] Old Dominion University, Norfolk, VA 23529

The On-Line Supporting Information (SI) includes:

(A) Materials and Methods

(B) Four Figures:

Fig. S1: Study of blue-shifts of LSPR spectra of single square-shaped NPs over their 12-week exposure to ambient conditions.

Fig. S2: Characterization of blue-shifts of LSPR spectra of single triangular NPs over their 12-week exposure to ambient conditions.

Fig. S3: Enlarged and high-resolution images of Fig. 4A in main text.

Fig. S4: Enlarged and high-resolution images of Fig. 5A in main text.

(C) References

¥ Both authors contribute equally to this work.
* To whom correspondence should be addressed: Email: xhxu@odu.edu; Tel/fax: (757) 683-5698; Email: helsayed@odu.edu; Tel: (757) 269-5645; Fax: (757) 269-5644

This journal is © The Royal Society of Chemistry 2011

Materials and Methods

Fabrication of Single Ag NP Arrays Using EBL

Single Ag NP arrays (25x25) were fabricated on microscopic glass slides coated with indium tin oxide (30-nm thickness) using EBL apparatus (ELPHY Quantum, Raith, Ronkonkoma) coupled with SEM (JSM-6060LV, JEOL). The slides (substrates) were spin-coated with polymethylmethacrylate (PMMA) positive photoresist, followed by EB exposure at 30 kV. The samples were developed in a developer with a ratio of methyl-isobutyl-ketone (MIBK) to isopropanol (IPA) at 1:3 for 30 s, and rinsed with IPA for 30 s to stop the development. The Ag thin films were deposited on PMMA-patterned slides using a standard thermal evaporation process at the deposition rate of ~0.5 Å/s to achieve desired thickness. The standard lift-off process was carried out to achieve the NPs with desired sizes, shapes and configured arrays. The inter-NP distances among neighboring individual NPs on the array were controlled at the minimal of 3.2-μm apart to eliminate potential dipole coupling of LSPR of individual NPs.

Characterization of Chemical, Structural and Plasmonic Properties of Single Ag NPs

The samples (microscope slides with EBL-fabricated single Ag NP arrays) were wrapped with Al-foil and placed under ambient conditions in the lab (air-conditioned dark room; 45-55% relative humidity; atmosphere; 25^0C) over 12 weeks. Individual NPs on the arrays were characterized in parallel using SEM/EDS, AFM (Dimension 3100, Veeco), and DFOMS.

Four corners of each array were marked with four different symbols using EBL, which can be easily recognized by all three imaging scopes (SEM, AFM, and DFOMS). This simple approach enables us to locate any given single NPs in the array, identify and characterize the same NP in each array using SEM, AFM and DFOMS to better understand chemical and

This journal is © The Royal Society of Chemistry 2011

morphological dependent LSPR spectra of single NPs over the duration of their exposure to the ambient conditions.

LSPR images and spectra of single NPs in the array were acquired simultaneously as the following. The deionized (DI) water was sandwiched between the nano-array microscopic slide and microscopic coverslip, which was then sealed to create a microchamber as the Xu group described previously.[1-3] LSPR images and spectra of single Ag NPs on each entire array on the slide immersed under the DI water were acquired individually and simultaneously in 5-100 milliseconds using DFOMS. Design and construction of DFOMS for characterization of single NPs were fully presented in our previous studies.[1-6] In this study, the dark-field optical microscope is equipped with a dark-field condenser (oil, 1.43-1.20), a microscope illuminator (Halogen lamp, 100 W), a 100x objective (Plan fluor 100x, N.A. 0.5-1.3), and Multispectral Imaging System (MSIS) (N-MSI-VIS-FLEX, CRI, CCD camera equipped with liquid-crystal tunable filter, LCTF).[7] The illumination power on the focal plane of dark field (sample stage) was measured as (0.070 ± 0.001) Watt using a power meter (Melles Griot)

References

1. X.-H. N. Xu, J. Chen, R. B. Jeffers and S. V. Kyriacou, *Nano Lett.*, 2002, **2**, 175-182.
2. Y. Song, P. D. Nallathamby, T. Huang, H. Elsayled-Ali and X.-H. N. Xu, *J. Phys. Chem. C.*, 2010, **114**, 74-81.
3. T. Huang and X.-H. N. Xu, *Nanoscale*, 2011, **3**, 3567-3572.
4. P. D. Nallathamby, T. Huang and X.-H. N. Xu, *Nanoscale*, 2010, **2**, 1715-1722.
5. P. D. Nallathamby, K. J. Lee, T. Desai and X.-H. N. Xu, *Biochemistry*, 2010, **49**, 5942-5953.
6. X.-H. N. Xu, W. J. Brownlow, S. V. Kyriacou, Q. Wan and J. J. Viola, *Biochemistry*, 2004, **43**, 10400-10413.
7. S. C. Gebhart, R. C. Thompson and A. Mahadevan-Jansen, *Appl. Opt.*, 2007, **46**, 1896-1910.

This journal is © The Royal Society of Chemistry 2011

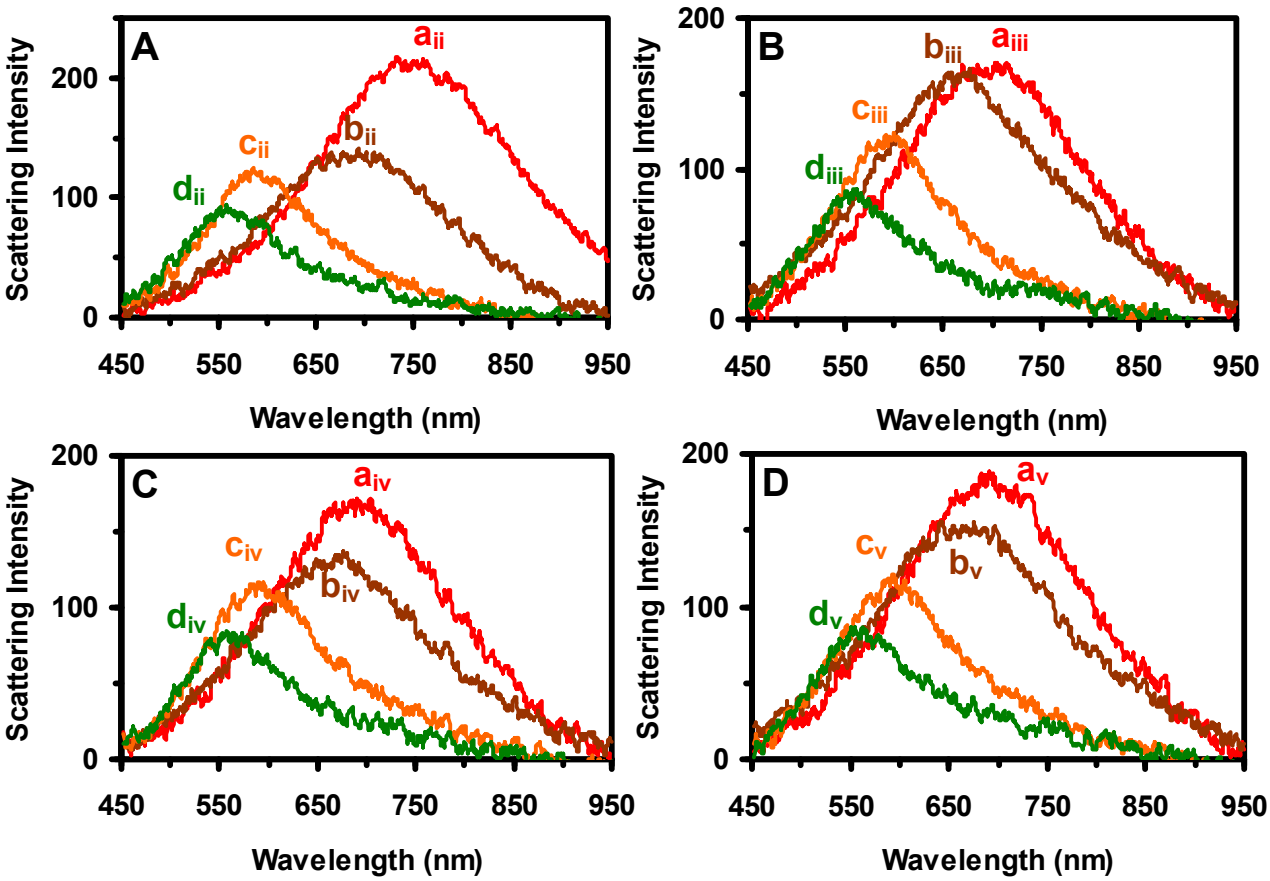


Figure S1: Study of the blue-shifts of LSPR spectra of single square-shaped NPs on the arrays marked as NP **(A)** (ii), **(B)** (iii), **(C)** (iv), and **(D)** (v) in Fig. 4B over their exposure to the atmosphere for **(a)** 0, **(b)** 1, **(c)** 4 and **(d)** 12 weeks. The λ_{max} (FWHM) of LSPR spectra of single NPs are: (a_{ii}) 733 (245), (b_{ii}) 666 (185), (c_{ii}) 586 (162), and (d_{ii}) 561 (126) nm for **(A)**; (a_{iii}) 738 (202), (b_{iii}) 659 (187), (c_{iii}) 600 (169), and (d_{iii}) 560 (127) nm for **(B)**; (a_{iv}) 720 (214), (b_{iv}) 653 (179), (c_{iv}) 595 (161), and (d_{iv}) 558 (122) nm for **(C)**; and (a_{v}) 692 (207), (b_{v}) 641 (188), (c_{v}) 594 (163), and (d_{v}) 562 (125) nm for **(D)**.

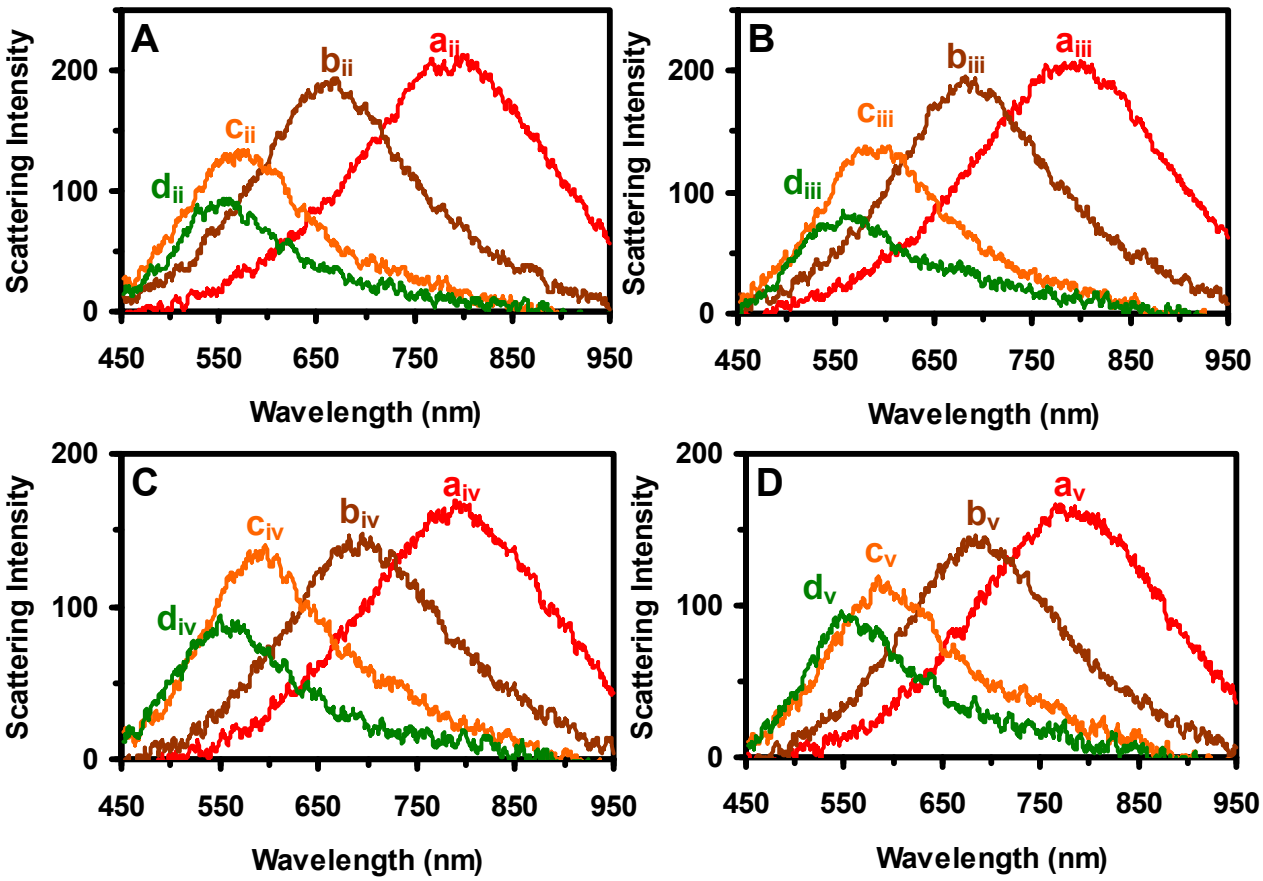
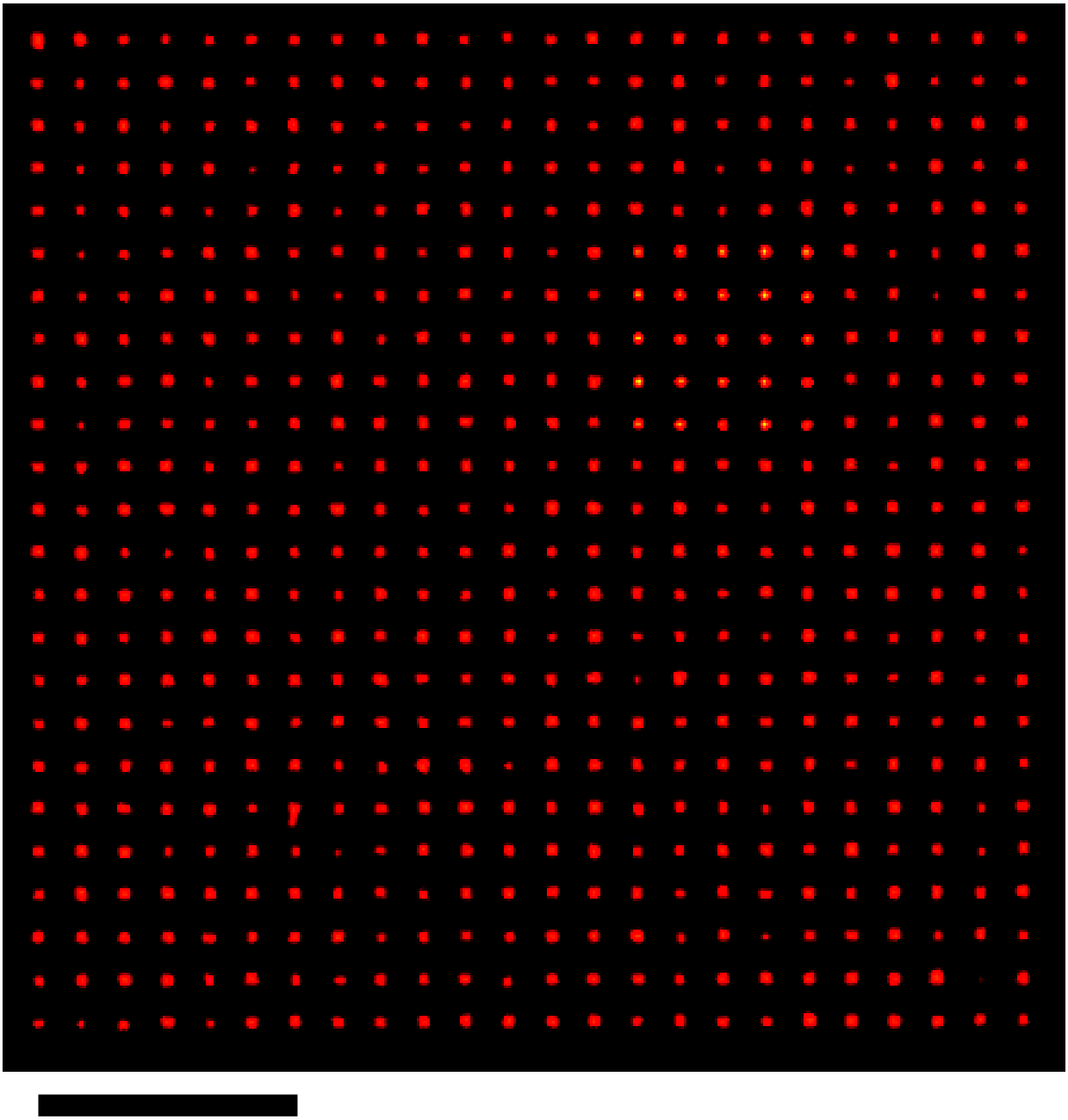


Figure S2: Study of the blue-shifts of LSPR spectra of single triangular NPs on the arrays labeled as NP **(A)** (ii), **(B)** (iii), **(C)** (iv), and **(D)** (v) in Fig. 5B over their exposure to the atmosphere for **(a)** 0, **(b)** 1, **(c)** 4 and **(d)** 12 weeks. The λ_{max} (FWHM) of LSPR spectra of single NPs are: (a_{ii}) 801 (263), (b_{ii}) 674 (218), (c_{ii}) 581 (169), and (d_{ii}) 561 (141) nm for **(A)**; (a_{iii}) 795 (258), (b_{iii}) 691 (215), (c_{iii}) 599 (183), and (d_{iii}) 557 (144) nm for (B); (a_{iv}) 793 (252), (b_{iv}) 701 (212), (c_{iv}) 598 (185), and (d_{iv}) 551 (143) nm for (C); (a_{v}) 774 (255), (b_{v}) 691 (188), (c_{v}) 593 (183), and (d_{v}) 548 (146) nm for (D).

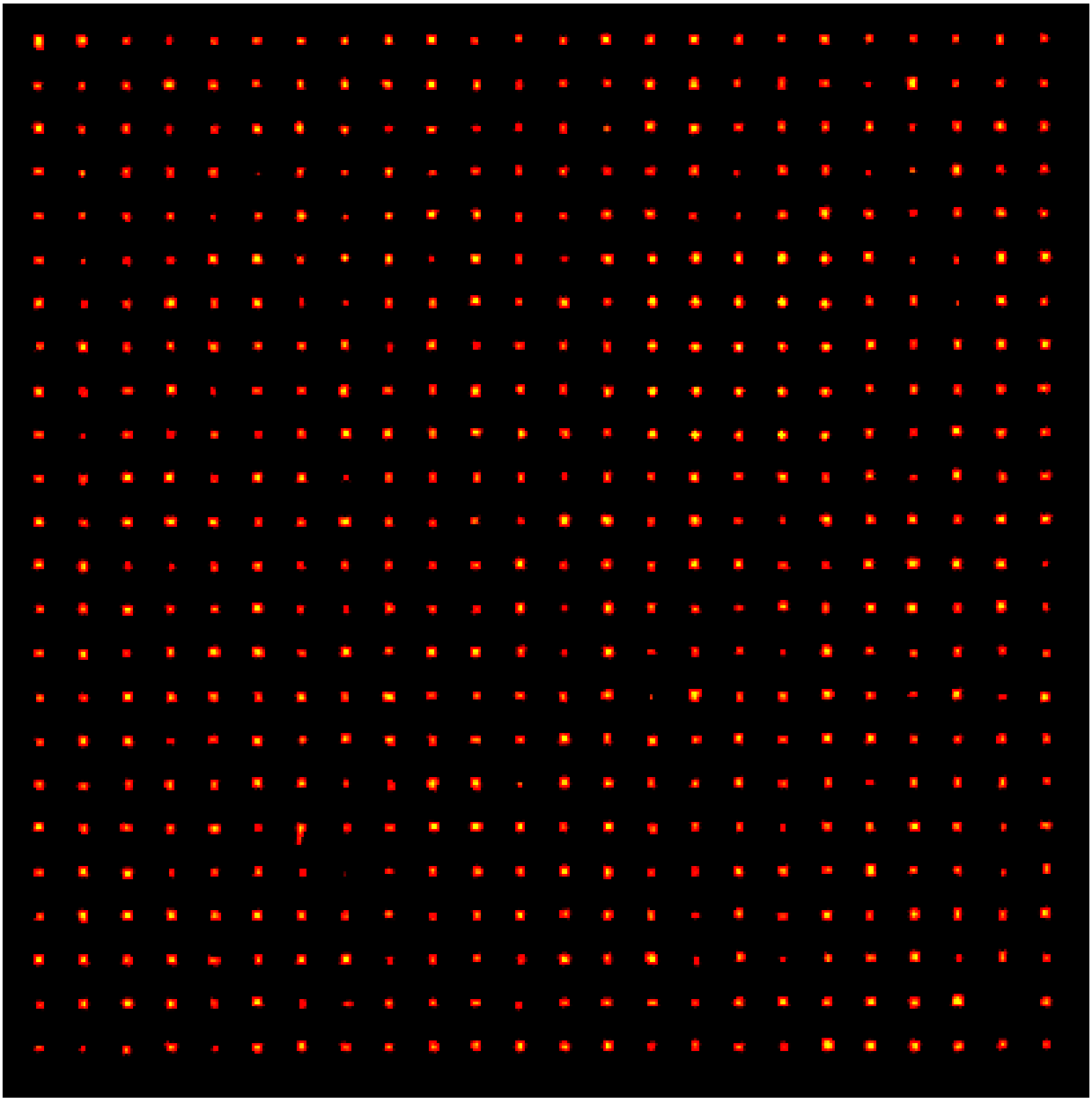
This journal is © The Royal Society of Chemistry 2011

Figure S3a



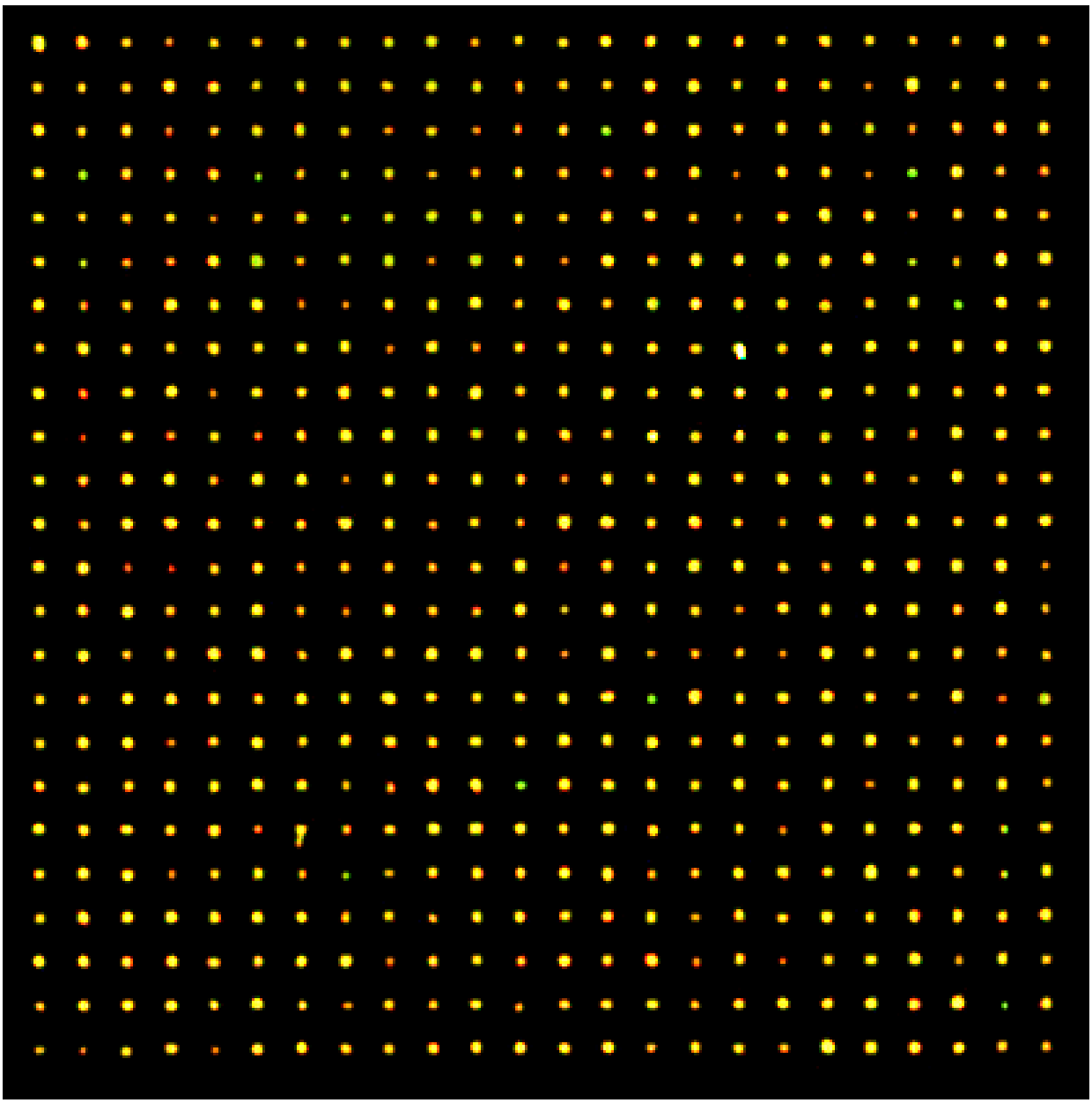
This journal is © The Royal Society of Chemistry 2011

Figure S3b



This journal is © The Royal Society of Chemistry 2011

Figure S3c



This journal is © The Royal Society of Chemistry 2011

Figure S3d

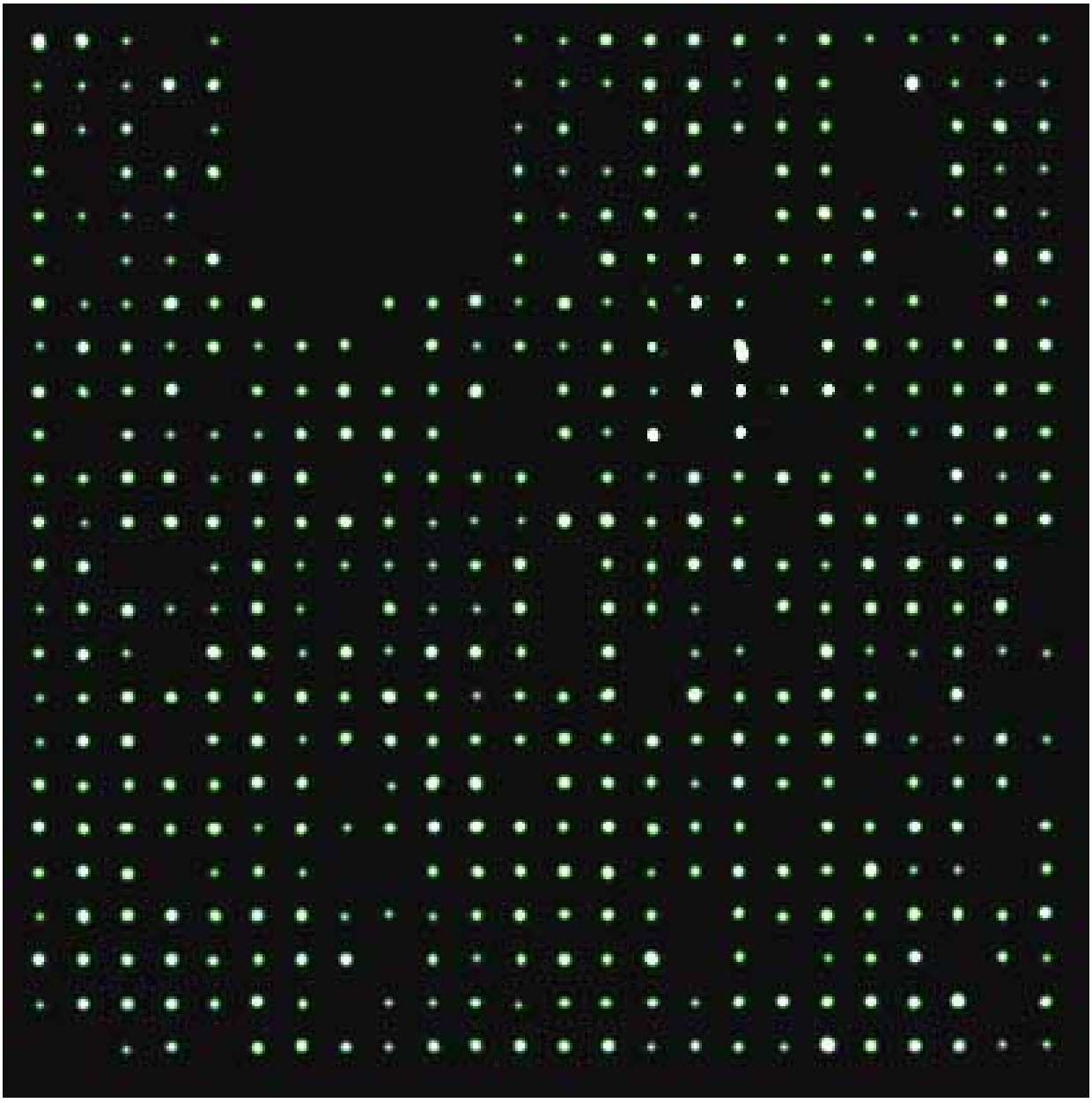
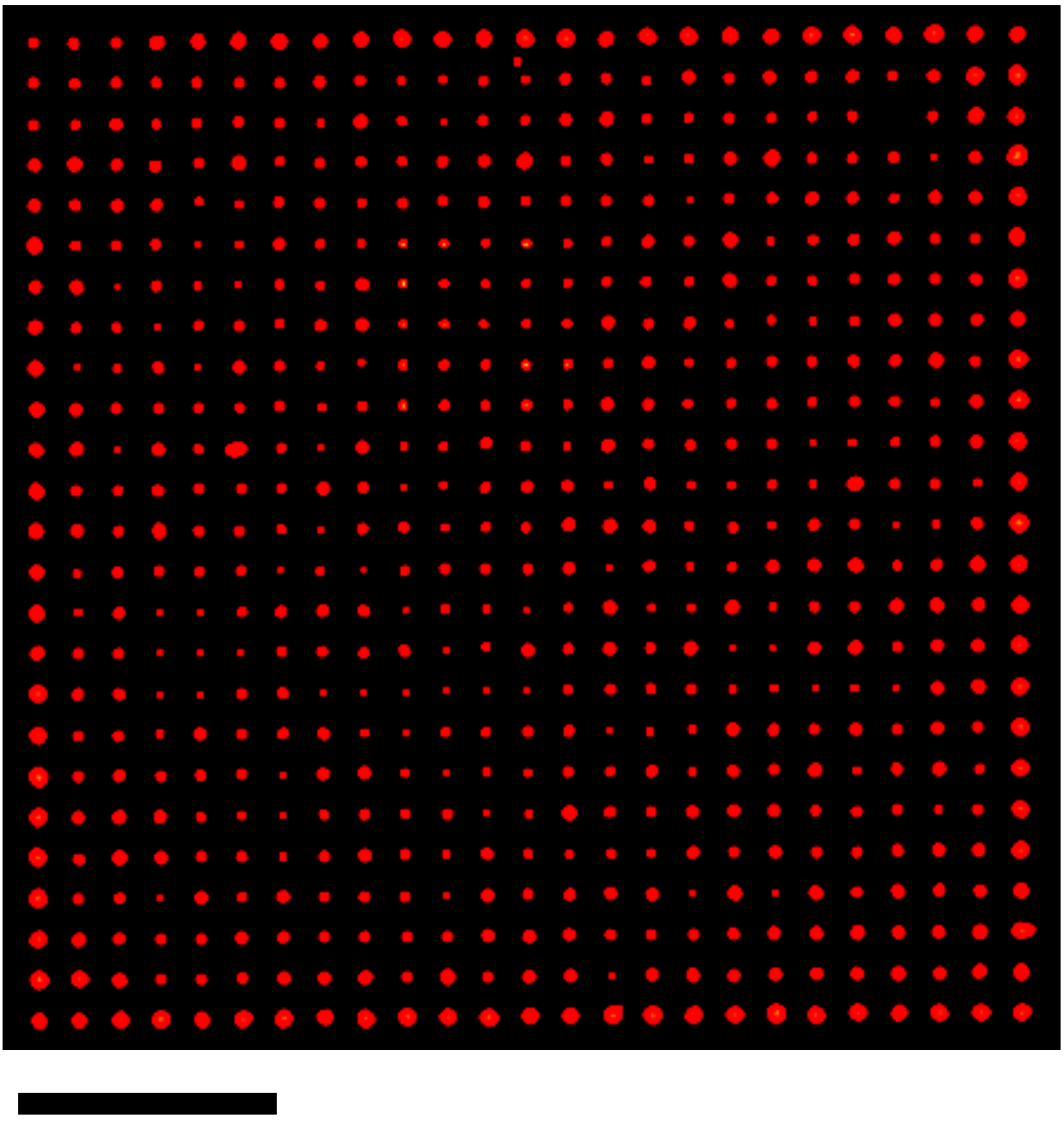


Figure S3: (a-d) Enlarged and high-resolution images of Figure 4A(a-d) in main text, respectively. Scale bars are 20 μm for all images.

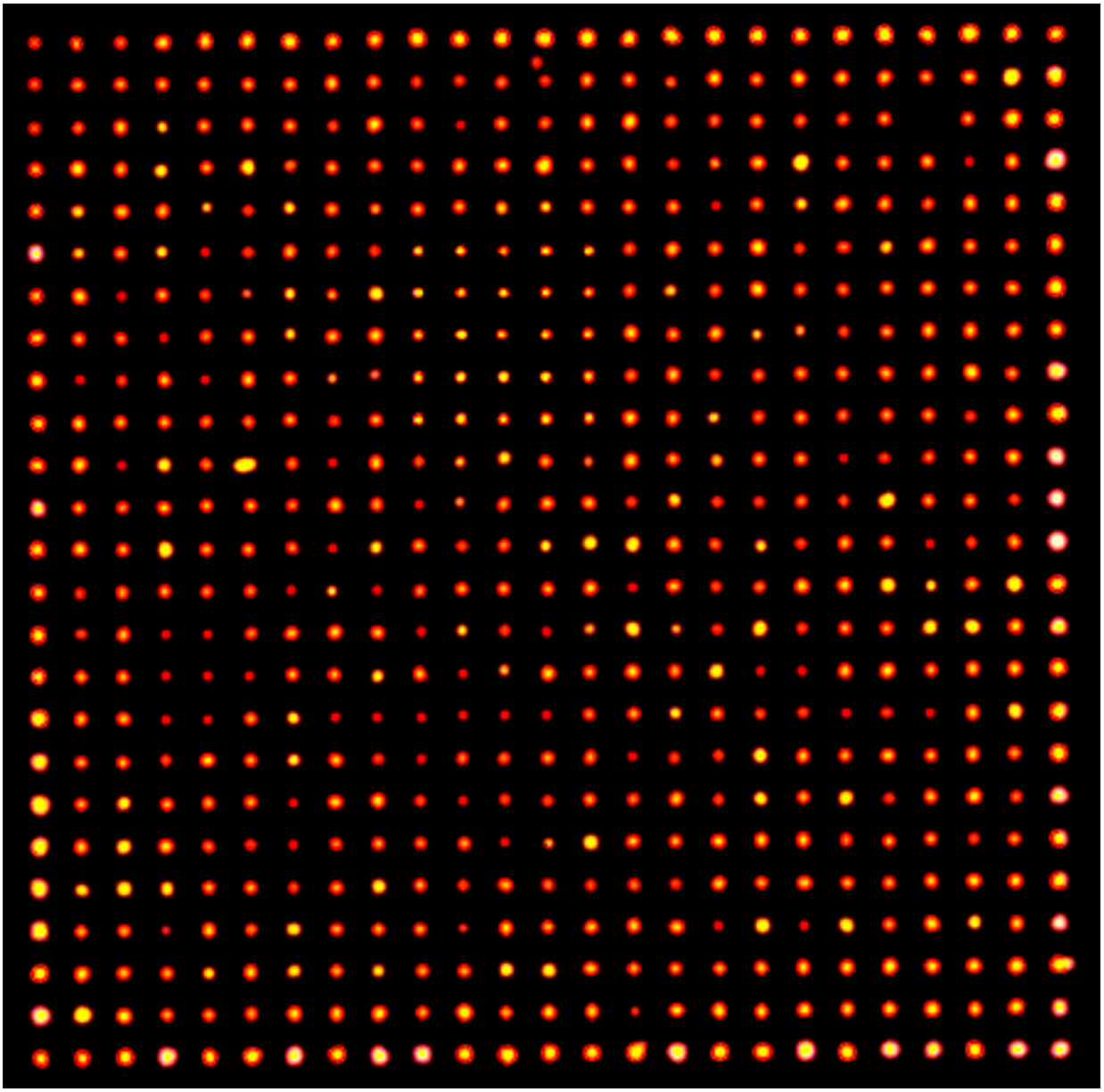
This journal is © The Royal Society of Chemistry 2011

Figure S4a



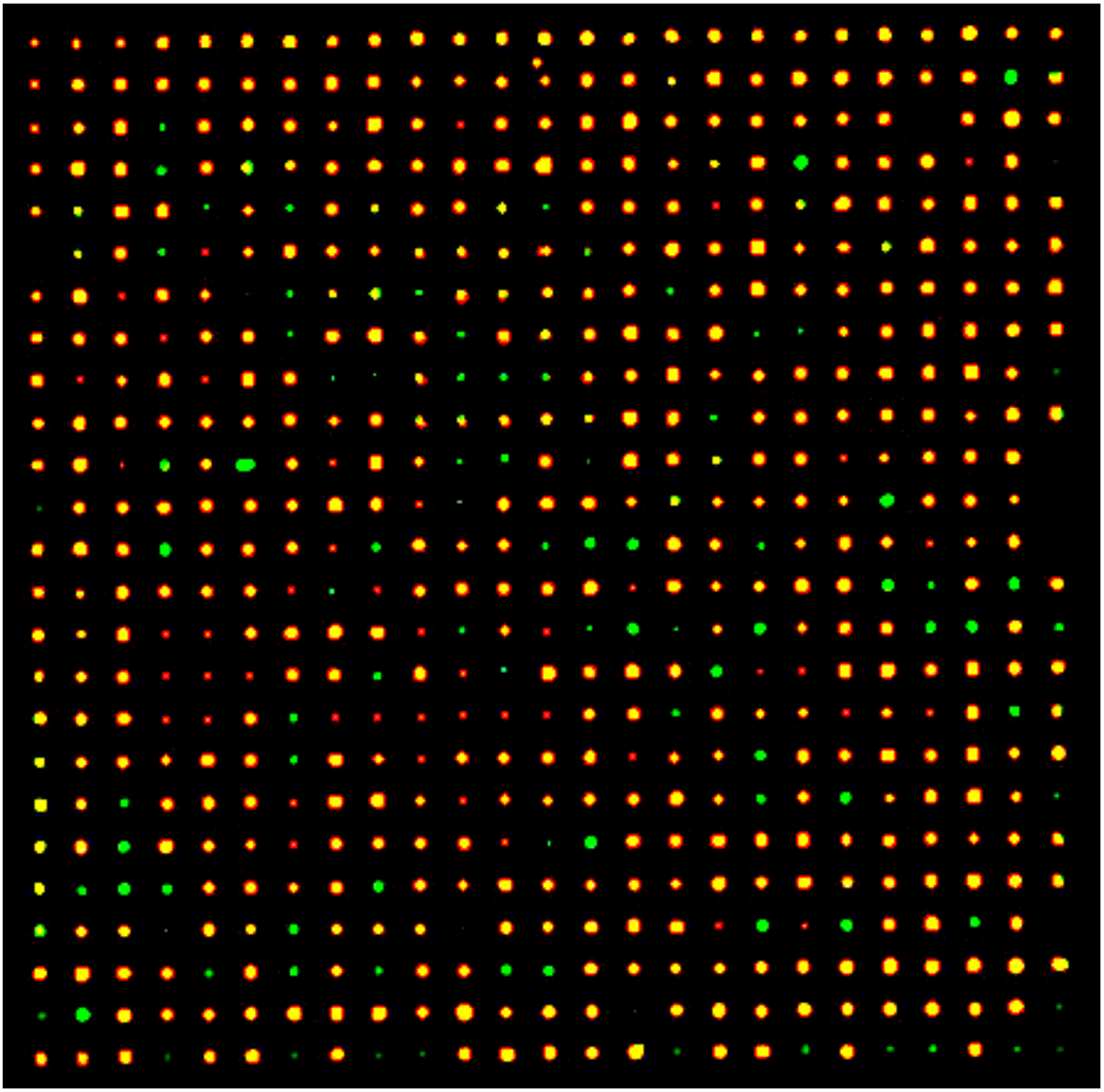
This journal is © The Royal Society of Chemistry 2011

Figure S4b



This journal is © The Royal Society of Chemistry 2011

Figure S4c



This journal is © The Royal Society of Chemistry 2011

Figure S4d

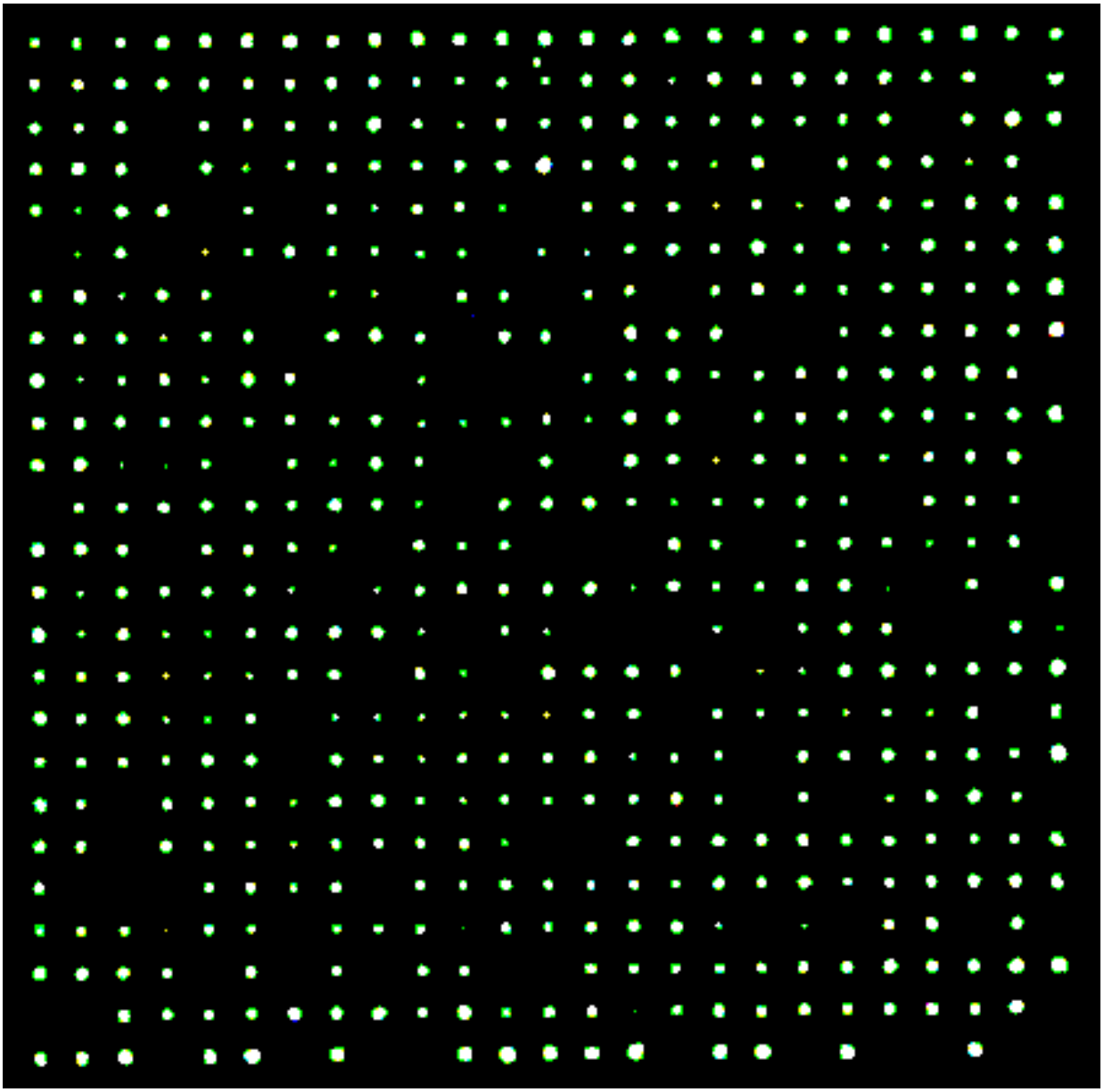


Figure S4: (a-d) Enlarged and high-resolution images of Figure 5A(a-d) in main text, respectively. Scale bars are 20 μm for all images.